

## Formation, Growth, and Properties of Atmospheric Aerosol Particles and Cloud Droplets

*Markku Kulmala, Ari Laaksonen, Pasi Aalto, Timo Vesala and Liisa Pirjola*

University of Helsinki, Department of Physics,  
P.O.Box 9 (Siltavuorenpenger 20D), FIN-00014 University of Helsinki, Finland

*Veli-Matti Kerminen, Pekka Korhonen, Risto Hillamo, Aki Virkkula and Minna Aurela*

Finnish Meteorological Institute, Air Quality Department,  
Sahaajankatu 20 E, FIN-00810, Helsinki, Finland

(Received: December 1995; Accepted: October 1996)

### *Abstract*

*Formation and growth of atmospheric aerosol particles and their physico-chemical properties have been examined using both aerosol and cloud models, and by conducting field experiments in the Finnish Arctic. Several routes for atmospheric particle production via homogeneous nucleation are proposed. Sulphuric acid - water nucleation is studied in more detail, and occasions of new particle production in the Finnish Arctic are identified. The bulk aerosol in the Finnish Arctic is rather acidic, with the least acidic particles originating from the ocean, and the most acidic ones from the East. We are able to show that the nucleation characteristics of these two types of particles are different. Acidic vapors are in addition shown to contribute to the formation and growth of cloud droplets strongly enough to change the optical thickness of an individual cloud under certain conditions.*

*Key words: aerosols, nucleation, cloud droplets, climate change*

### *1. Introduction*

The increasing atmospheric concentrations of greenhouse gases, such as carbon dioxide and methane, can potentially drive a significant warming of the Earth's climate (IPCC, 1990, 1992, 1994). However, much attention has recently been paid to the globally increased backscattering of solar radiation due to enhanced aerosol particle concentrations. This phenomenon may reduce considerably the warming effect of greenhouse gases in the atmosphere (Charlson *et al.*, 1991, 1992; Charlson and Wigley, 1994).

Atmospheric aerosol particles influence the Earth's radiation balance both directly by scattering and absorbing solar radiation, and indirectly by acting as cloud condensation nuclei (CCN). Increased aerosol and CCN concentrations lead not only to increased scattering of light back to space, but also to higher cloud albedos. Enhanced

CCN concentrations can also lead to increased cloud lifetimes, for which some observational evidence exists (*Parungo et al.*, 1993). Greater cloud lifetimes affect undoubtedly atmospheric radiation fluxes, but the magnitude or even the sign (heating or cooling) of this effect is very difficult to estimate (e.g. *Penner et al.*, 1994).

The direct aerosol-climate interaction has been studied more intensively than the indirect one. The most recent simulations using General Circulation Models (GCM) show that observed changes in global climate parameters can be predicted more accurately when direct (sulphate) aerosol forcing is included (*Mitchell et al.*, 1995). However, current numerical studies do not include all climatically relevant aerosol types, and the most important formation routes for new particles are still under study. Thus, a considerable improvement in our understanding of particle formation processes is needed before we are reliably able to predict the influences of aerosol particles on the global climate.

Numerical GCM experiments have also been performed to estimate the indirect aerosol-climate interaction (e.g. *Erickson et al.*, 1995). Since clouds cover approximately 50 % of the Earth's surface, even minor changes in their reflectivity at solar wavelengths may be significant. The ability of aerosol particles to act as CCN depends on their size and chemical composition. In addition to sulphate, also many other inorganic and organic compounds may contribute to CCN production (*Kulmala et al.*, 1993; *Novakov and Penner*, 1993; *Wurtzler et al.*, 1995). The prediction of CCN concentrations in the real atmosphere, where the size distribution and the composition of particles may vary vastly, is still a very hard task. According to measurements, the relationship between elevated aerosol particle concentrations and the number of cloud droplets seems to be highly non-linear (e.g. *Leitch et al.*, 1992).

Evidently we do not understand the phenomena controlling atmospheric CCN concentrations well enough; there is at the moment neither a theoretical nor an empirical basis for global modelling of the indirect aerosol effect (*Penner et al.*, 1994). The lack of a rigorous treatment of this effect in climate models is a serious shortcoming, since it may be more important than the direct aerosol effect (*Kaufman and Chou*, 1993). Thus, it is of great importance to improve our understanding of the phenomena controlling atmospheric CCN and the resulting cloud droplet number concentrations.

In the present paper a summary of the aerosol-cloud-climate related studies performed during the SILMU-project is given. First we offer an overview on the formation and growth of atmospheric aerosol particles, after which some field data from the Finnish Arctic is presented. Finally we introduce results from our most recent studies concerning the interaction between the atmospheric particle and trace-gas concentrations, and the formation and growth of cloud droplets.

## 2. Formation and physico-chemical transformation of atmospheric aerosol particles

### 2.1 General structure of atmospheric particle size distribution

Atmospheric aerosol particles are divided into two major size categories, coarse (particle diameter  $> 1 \mu\text{m}$ ) and fine ( $< 1 \mu\text{m}$ ). Coarse particles originate mainly in natural processes like mechanical disintegration of crustal material and bubble bursting over ocean surfaces. The climatically more important fine particles are largely of anthropogenic origin and are often transformed greatly in the atmosphere.

Fine, or submicron, particles exhibit three separate size modes: nuclei, Aitken and accumulation modes. The removal resistant accumulation mode is located between  $0.1$  and  $1 \mu\text{m}$  in particle diameter, and it is found in all atmospheric air masses. The presence of a nuclei mode, the size of which ranges from a few nanometers to some  $10\text{--}20 \text{ nm}$ , is a sign of a recent nucleation event in the atmosphere. The Aitken mode is located between the nuclei and accumulation modes. An example of a particle number size distribution measured over the Arctic Ocean is shown in Figure 1. In the Figure, all three submicron modes can be identified (*Wiedensohler et al.*, 1996).

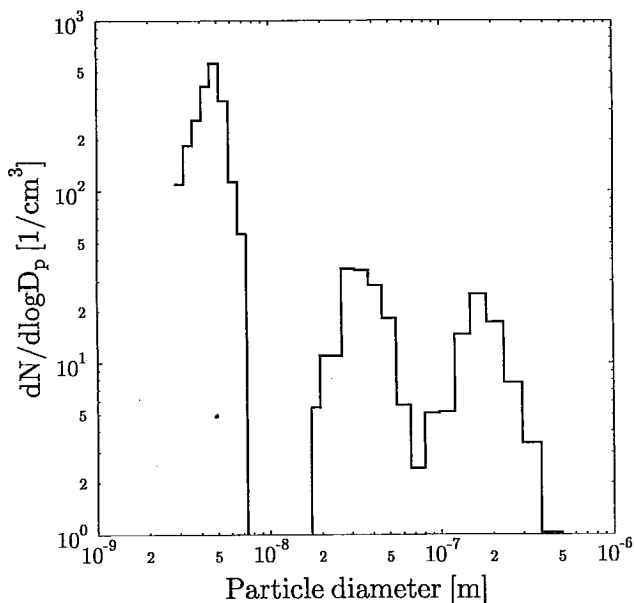


Fig. 1. Typical three-modal particle number size distribution.

Depending on atmospheric conditions, particle number concentration may peak in either nuclei, Aitken, or in the accumulation mode. This is in contrast to particulate

mass, most of which is found in the accumulation and coarse particle size ranges. Examples of chemical particle mass size distributions are shown below, in section 3.2.

## 2.2 New particle production in the atmosphere

In addition to primary particles emitted directly from various sources, there are secondary particles formed from gaseous precursor species in the atmosphere. Observations of secondary particle production have been reported in several kinds of different aerosol systems, including power plant plumes (*Van Valin and Pueschel, 1981*), remote marine areas of little anthropogenic influence (*Hoppel et al., 1994*), and Arctic and Antarctic regions (*Sheridan, 1989; Gras, 1993*).

There is strong evidence that atmospheric particle production takes place via multicomponent routes of homogeneous nucleation. According to both theory and field experiments, potential nucleation pathways in the atmosphere are those between the following vapor species: I)  $\text{H}_2\text{SO}_4 - \text{H}_2\text{O}$ , ii)  $\text{HCl} - \text{NH}_3$ , iii)  $\text{H}_2\text{SO}_4 - \text{NH}_3 - \text{H}_2\text{O}$ , iv)  $\text{HCl} - \text{NH}_3 - \text{H}_2\text{O}$ , v) ions -  $\text{H}_2\text{SO}_4 - \text{H}_2\text{O}$ . Some secondary organic vapors may also participate in nucleation, but the role of these compounds remains to be studied in the future.

Traditionally, the route (i) has been believed to be the dominant one in the troposphere, and it has also been studied most widely (e.g. *Raes and Van Dingenen, 1992; Russell et al., 1994; Kulmala et al., 1995b*). However, in the light of laboratory studies (*Wysloutzil et al., 1991*), this mechanism may often not be efficient enough to explain observed atmospheric concentrations of fresh sulphate particles. The route (ii) is well known (*Countess and Heicklen, 1973; Henry et al., 1983*), but according to present nucleation theories (*Seinfeld, 1986; Girshick et al., 1990*) it does probably not produce new particles under atmospheric conditions at temperatures above  $-20^\circ\text{C}$  (*Kulmala et al., 1995c*). The routes (iii) and (iv), combining a chemical reaction between an acid and ammonia and the dilution effect of water, are most likely more effective than the respective routes without ammonia (i and ii) (*Coffman and Hegg, 1995*). It has been proposed recently that ions produced by solar UV radiation may speed up sulfate nucleation (*Raes and Van Dingenen, 1992; Hoppel et al., 1994*), and therefore also route (v) might be possible under certain atmospheric conditions.

The rate at which new particles are being produced in the atmosphere depends on the production of condensable vapours, on the ambient temperature and relative humidity, and on the characteristics of pre-existing aerosol particles such as their number concentration, size distribution and chemical composition. Therefore, it is important to examine what are the atmospheric conditions under which the production of new particles will significantly change the number and thereby the dynamics of aerosol particles. Using computer simulations, *Kulmala et al. (1995b)* have derived an analytical expression to estimate whether particle production via route (i) is significant under given ambient conditions. This straightforward parametrisation gives the nucleation efficiency as a function of relative humidity, temperature, OH and  $\text{SO}_2$

concentrations, as well as of the size and concentration of pre-existing particles. We will use this parametrization below in Section 3.3 to show that certain nucleation events in the Finnish Lapland, connected to pollution from the Kola Peninsula, can be explained by route (i).

### 2.3 Growth of atmospheric aerosol particles

Once emitted as primary or formed as secondary, submicron aerosol particles grow by a number of processes prior to their removal from the atmosphere. These processes include condensational mass transport between the gas and particulate phases, coagulative growth of particles, aqueous-phase reactions in cloud or fog droplets, and inter-phase reactions on the surface or inside the particles.

Excluding sulfate which is formed predominantly via heterogeneous pathways, most secondary particulate matter is due to condensation of various inorganic and organic vapors onto the particulate phase. Although the kinetics of condensation is well known, large uncertainties related to the accommodation of condensing vapors on particle surfaces, and to the thermodynamics dictating the equilibrium between the gas and particulate phases, still exist. Condensational mass transport favors the growth of smallest particles; accumulation-mode or greater particles are unlikely to grow much by condensation (*Kerminen and Wexler, 1995b*).

Coagulation, while efficiently depleting small nuclei from the air, requires particle concentrations of the order  $10^6 \text{ cm}^{-3}$  or greater to significantly contribute to particle growth (*Kerminen and Wexler, 1995a*). These high concentrations are possible but not very common in the planetary boundary layer, which generally allows us to neglect coagulation in aerosol models. The situation may be different in mid or upper free troposphere, where both particle number concentrations and their residence time often are higher (*Raes, 1995*).

Aqueous-phase reactions in cloud and fog droplets convert dissolved sulphur dioxide to sulphate, being responsible for a large fraction of the fine particulate matter in a global scale (*Langner and Rodhe, 1991*). Processing of air through non-precipitating clouds increases rapidly the residual particle size, especially for the smallest activated particles. As a result particles from the upper end of the Aitken mode move into the accumulation mode, and a gap between these two modes is created (*Hoppel et al., 1994; Kerminen and Wexler, 1995b*).

Inter-phase reactions are known to participate in many atmospheric phenomena, including the formation of ozone hole in the polar stratosphere (*Hofmann et al., 1989*), the release of chloride from sea salt particles (*Karlson and Ljunström, 1995*), and the reaction of  $\text{SO}_2$  with different kinds of aerosol particles (*De Santis and Allegrini, 1992*). Due to complicated nature of heterogeneous chemistry, however, the role of inter-phase reactions in particle growth has remained uncertain.

### 3. Chemical and physical characteristics of aerosol particles in the Finnish Arctic

#### 3.1 Experimental evidence of tropospheric particle production

The formation of new aerosol particles in arctic conditions has been observed several times during the measurements performed between June 1993 and August 1994 in Värriö environmental measurement station (67° 50'N, 29° 35'E, see Fig. 2).

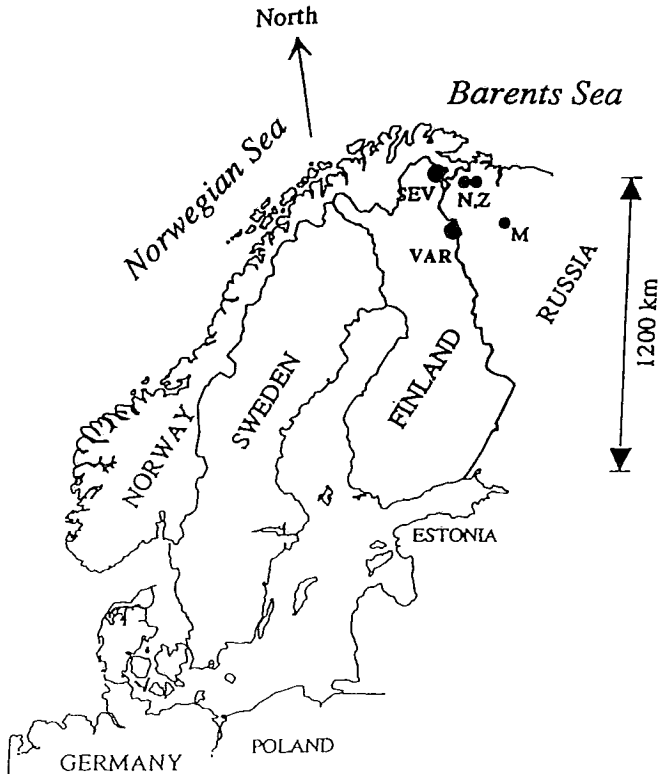


Fig. 2. Locations of Sevettijärvi (SEV) and Värriö (VAR) stations. Significant pollution sources are Nikel (N), Zapoljarnyi (Z) and Monchegorsk (M).

Particle size distributions were measured using a TSI diffusion battery model 3040 and a condensation nucleus counter model 3022. Gaseous  $\text{SO}_2$  and  $\text{O}_3$  and meteorological parameters were monitored simultaneously. The average particle concentration during this period was  $1170 \text{ cm}^{-3}$ , with a maximum of  $24000 \text{ cm}^{-3}$  and a minimum of  $33 \text{ cm}^{-3}$ . The particle mean size was 82 nm and GSD (Geometric Standard Deviation) 3.0. This agrees quite well with earlier measurements during the spring of 1992 when DMPS (Differential Mobility Particle Sizer) system was used for one week.

In 1992 two or sometimes three particle modes were found. The accumulation mode was located at 180 nm, with a mean particle concentration of  $290 \text{ cm}^{-3}$  and GSD of 1.5. Aitken-mode particles were located around 40 nm with a mean concentration of  $530 \text{ cm}^{-3}$  and GSD of 1.7. Moderate bursts of new particles with diameters around 10 nm were also observed. Two typical size distributions from this measurement period are presented in Figure 3. The first of them shows typical clean-air conditions with a small Aitken mode. The second size distribution with a large nucleation mode was measured during a pollution event from the Kola Peninsula.

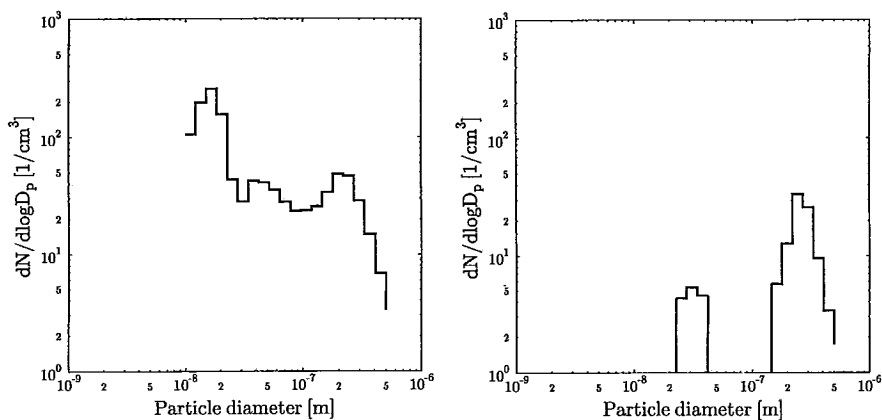


Fig. 3. Particle size distributions with high and low nucleation mode particle concentrations.

Diffusion battery measurements were analyzed with Extreme Value Estimation (EVE) (Aalto *et al.*, 1990). Particles were classified in the following three different size classes:  $D_p < 30 \text{ nm}$ ,  $30 \text{ nm} < D_p < 90 \text{ nm}$  and  $D_p > 90 \text{ nm}$ . Although high  $\text{SO}_2$  concentrations originate from the Kola Peninsula, high particle concentrations have no wind direction dependency. Accumulation- and Aitken-mode particles have an annual maximum during the summer, and nucleation-mode particles during the spring. The lowest particle and  $\text{SO}_2$  concentrations enter Lapland from the Norwegian Sea. There is no real correlation between  $\text{SO}_2$  and nucleation-mode particle concentrations, but when incidents with the mean particle size smaller than 20 nm are selected, the correlation becomes higher. The correlation between nucleation mode particles and ozone is actually higher than that with  $\text{SO}_2$  because they both have spring maxima. The analysis of trajectories (Aalto *et al.*, 1995) shows that the events with both high  $\text{SO}_2$  and particle concentrations are typical of air masses coming from the Kola Peninsula. However, there are situations where nucleation-mode particle concentration is high but  $\text{SO}_2$  concentration below the detection limit ( $0.2 \mu\text{g}/\text{m}^3$ ). In these cases air masses have come from the Norwegian Sea.

### 3.2 Chemical composition and other properties of aerosol particles

Since spring 1992, aerosol properties have been monitored continuously at the Sevettijärvi station (69° 35'N, 28° 50'E, see Fig. 2). The site is located near the Arctic Ocean some 30 km from the closest bay of the Barents Sea. At the moment, measurements in Sevettijärvi include the monitoring of the basic meteorological parameters (temperature, relative humidity, and wind speed and direction), particle concentration above the 14-nm size and in two narrower size regimes ( $0.3 < D_p < 0.5 \mu\text{m}$  and  $D_p > 0.5 \mu\text{m}$ ), aerosol scattering and backscattering coefficients, and gaseous  $\text{SO}_2$ ,  $\text{NO}_2$  and  $\text{O}_3$ . Particle chemical composition is measured continuously using a 2-stage virtual impactor, and during more extensive field campaigns using a 11-stage Berner low pressure impactor (BLPI). Species analyzed from the impactor samples include the major inorganic compounds and methanesulfonic acid (MSA) - a tracer for biogenic sulfur emissions from the oceans.

Examples of BLPI-based data are shown in Figure 4, where mass size distributions of sulphate, ammonium and sodium are presented. The continuous distributions are extracted from the raw impactor data using the inversion code MICRON (Wolfenbarger and Seinfeld, 1990), with the collection efficiency curves of the impactor stages needed by the code taken from Hillamo and Kauppinen (1991). The period A in Figure 4 represents a case where measured air masses originated mostly from the Arctic Ocean, and arrived at Sevettijärvi via northern Scandinavia. As a result a dominant sodium mode indicative of sea-salt particles can be seen in the coarse particle size range. During the period B, air masses come mainly from Russia and have little contact with an open ocean. This leads to a negligible amount of sodium compared to mostly anthropogenically-derived sulphate. The tails in sulphate and ammonium size distributions in the Aitken mode are due either to very small primary particles, or to particles born and grown during their transport to Sevettijärvi.

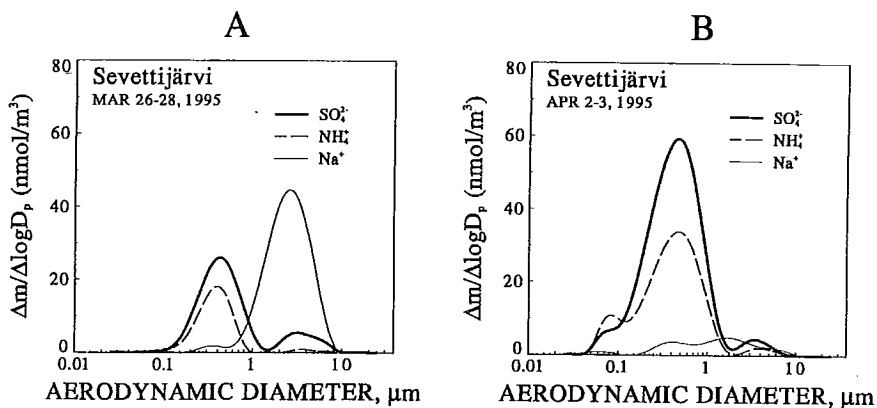


Fig. 4. Particle mass size distributions measured in Sevettijärvi in the Finnish Arctic.



On an annual base, sulphate and ammonia contribute to some 40 % of the dry, submicron particle mass in Sevetijärvi (*Virkkula et al.*, 1995). The proportions of fine-particle sulphate and ammonium between the wind sectors, together with that of the sulphate precursor gas  $\text{SO}_2$ , are shown in Figure 5. As one can see, most  $\text{SO}_2$  comes from the East and can be ascribed to the large pollution sources of Nickel and Zapolyarnyi areas in the Kola Peninsula.

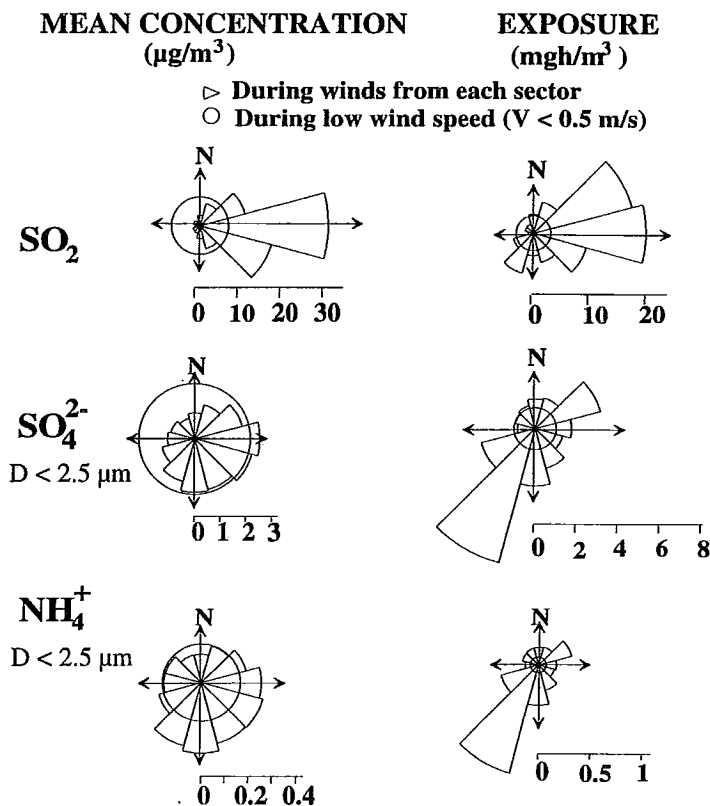


Fig. 5. The concentration and exposure of  $\text{SO}_2$  and of fine-particle sulphate and ammonium in Sevetijärvi, as averaged over the period January 1992 - July 1994 and distributed between the different wind sectors.

Atmospheric  $\text{SO}_2$  oxidation rates are smaller than a few per cent per hour, so only a minor fraction of  $\text{SO}_2$  from the Kola Peninsula can be converted to sulphate prior to its arrival at Sevetijärvi. The prevailing wind direction in Sevetijärvi is SW, which is also where most sulphate and ammonium come from. According to trajectory statistics, the main source areas for ammonium observed in Sevetijärvi are in western Europe, whereas sulphate originates more evenly from the whole continental Europe (*Virkkula et al.*, 1995).

Regardless of the air mass origin, the submicron aerosol in Sevetijärvi is acidic. This reflects the lack of local and nearby ammonia sources. The most acidic particles with average anion to cation ratios above 2 are found in wind sectors E-SE. More marine-related wind sectors, W-N, exhibit average anion to cation ratios between 1.4 and 1.6.

Aerosol scattering coefficient in Sevetijärvi has a maximum in March (geometric mean  $1.8 \cdot 10^{-5} \text{ m}^{-1}$ ), and a minimum in April ( $8.1 \cdot 10^{-6} \text{ m}^{-1}$ ). Although the seasonal cycle is discernible, it is much weaker than that in high Arctic sites experiencing strong spring-time haze episodes. The mean scattering coefficient in Sevetijärvi is of the same order as that at Ny Ålesund in the Norwegian Arctic ( $79^\circ \text{ N}$ ,  $12^\circ \text{ E}$ ) or at Barrow in Alaska ( $71^\circ \text{ N}$ ,  $157^\circ \text{ E}$ ), but over a magnitude greater than that observed in the South Pole (Bodhaine, 1983).

### 3.3 Analysis of two nucleation events in Lapland

The measurements in both Värriö and Sevetijärvi have shown that two kinds of nucleation events can be observed in the Finnish Arctic, one group of fresh particle populations originating from the pollution from the Kola peninsula, and the other originating from the Arctic Ocean. Even though both types of particles are acidic and contain substantial amounts of sulphur, their nucleation mechanisms most probably are different. We will show below, that an observed pollution nucleation event can be explained theoretically with a binary nucleation mechanism of sulphuric acid and water, the acid being produced by gas phase chemistry of  $\text{SO}_2$  and OH-radicals. However, it is not possible to explain theoretically a nucleation event taking place in marine air with the same mechanism. Our approach is based on calculation of binary nucleation rates along the trajectories leading to Värriö station at the times of the two observed events of high concentrations of fresh particles, and comparison of the calculated and measured aerosol concentrations.

The formation of gaseous sulphuric acid, and the nucleation of new sulphuric acid-water particles were simulated by an integrated model incorporating an atmospheric gas-phase chemistry model (Pirjola, 1995) and a three-mode (nucleation, Aitken, and accumulation) integral aerosol dynamics model (Kulmala et al., 1995b). The chemistry model is a trajectory-based air quality model. A well-mixed column of air with a height of 1000 m, moves along the wind trajectory and picks emissions from different sources. For each atmospheric species (67 altogether) chemical loss and production, emission and deposition are taken into account. The most relevant species to sulphuric acid formation are hydroxyl radicals and sulphur dioxide. In the case of the marine nucleation event, the concentrations of both OH-radicals and  $\text{SO}_2$  were simulated along the trajectory. However, in the case of the pollution event we relied on  $\text{SO}_2$  observations made in Värriö.

The integral aerosol model accounts for nucleation, and condensation of sulphuric acid and water onto pre-existing particles. The initial Aitken-mode particle

concentrations were assumed to be  $10 \text{ cm}^{-3}$  in the marine case and  $1000 \text{ cm}^{-3}$  in the pollution case. Because meteorological data associated with the trajectories was not available, the temperatures and relative humidities measured in Värriö were used as approximations in both cases. We assumed clear sky conditions, with the albedo being 0.8 (snowy conditions) in both cases.

The largest uncertainties in the aerosol model are related to the calculation of the nucleation rate (*Laaksonen et al.*, 1995), and to the sticking probability of condensing molecules. Luckily, in the particular conditions considered here, the theoretical nucleation rates are very close to those extrapolated from the experimental work of *Wyslouzil et al.*, (1991).

The nucleation events selected took place on February 25 and April 11, 1994, respectively. In the former case the air trajectory came from northeast via the Kola peninsula, sulphur dioxide concentration was high ( $19.9 \mu\text{g}/\text{m}^3$ ), the total particle concentration was  $8400 \text{ cm}^{-3}$ , and the concentration of Aitken and accumulation mode particles about  $1000 \text{ cm}^{-3}$ . In the latter case the air trajectory came from the Arctic Sea through Norway, observed sulphur dioxide concentration was low (below  $0.25 \mu\text{g}/\text{m}^3$ ), the total particle concentration was around  $3300 \text{ cm}^{-3}$ , and concentration in Aitken and accumulation modes about  $1000 \text{ cm}^{-3}$ . Temperatures were  $-12.9$  and  $2.4^\circ$ , and relative humidities 70.5% and 50%, respectively.

The simulated nucleation mode particle concentrations in the marine case (April) were essentially zero. This suggests that the high particle concentrations of 11 April were not produced by binary nucleation of sulphuric acid (produced by gas-phase chemistry) and water. Either some other chemical species have participated in the nucleation event, or there has been high concentrations of sulphuric acid in the gas phase due to evaporation from pre-existing acidic particles (*Eisele and Tanner*, 1993).

The simulation of the nucleation event of 25 February shows different characteristics. The OH times  $\text{SO}_2$  concentration is above the level of theoretical requirement for sulphuric acid production to be high enough for binary nucleation to take place. The simulated nucleation mode concentration is  $5300 \text{ cm}^{-3}$ , comparing very well with the measured value. However, it has to be borne in mind that there are factors causing uncertainty in the calculations. One of these is the theoretical nucleation rate used. Temperature and relative humidity should be calculated along the trajectory. Furthermore, possible cloudiness affects the OH concentrations, and should be accounted for. In the future, we will try to minimize the uncertainty related to these factors in our simulations.

#### 4. Formation of Cloud Droplets

The formation of cloud droplets occurs on pre-existing aerosol particles. The number and size of cloud droplets is affected strongly by the size distribution of pre-existing particles, as well as by their chemical composition. Field experiments show that atmospheric aerosol particles usually consist of both hygroscopic and insoluble

components (Zhang *et al.*, 1993; Svenningsson *et al.*, 1992, 1994). According to our model studies, the soluble mass of pre-existing aerosol particles together with growth dynamics are the most important factors in the droplet activation process (Korhonen *et al.*, 1996a, 1996b; Kulmala *et al.*, 1996). This is due to the fact that hygroscopic substances lower the water vapour saturation pressure over particle surfaces, hence alleviating the droplet activation.

In our recent studies we have explored how condensable trace gases (HNO<sub>3</sub> and HCl in our examples) influence the cloud droplet number concentrations due to the increased amount of hygroscopic matter in developing CCN (Kulmala *et al.* 1993, 1995a, d; Korhonen *et al.* 1996a, b). For the description of the cloud environment, an adiabatic air parcel model has been used. We have also applied an entraining air parcel model to examine the influence of entrainment of drier air during the activation process. Cloud dynamics (e.g. different air updraft velocities) has been identified to be an important factor (Kulmala *et al.*, 1993; Korhonen *et al.*, 1996a).

In our latest studies (e.g. Kulmala *et al.*, 1996), we have developed the microphysical model further and concentrated especially in the description of the initial aerosol particle distribution. In this context a realistic four-mode particle distribution has been applied: two modes in both size and hygroscopicity, i.e. more and less hygroscopic particles in both Aitken and accumulation modes (Kulmala *et al.*, 1996). The results from a series of simulations can be summarized using the following expression to connect cloud droplet concentration ( $N$  in cm<sup>-3</sup>) with the initial aerosol particle ( $P$  in cm<sup>-3</sup>) and gaseous nitric acid ( $C$  in ppbv) concentrations:

$$\ln N = \alpha + \beta \ln P + \gamma \ln C \quad (1)$$

Here  $\alpha$ ,  $\beta$ ,  $\gamma$  are constants.

The fitting was performed using the data obtained in our recent study (Kulmala *et al.*, 1996). The constants ( $\alpha$ ,  $\beta$ ,  $\gamma$ ) have the values 0.6108, 0.6381 and 0.0465, respectively, when the air updraft velocity ( $w$ ) is 0.1 m/s. In the case of  $w = 1.0$  m/s, the respective values are 0.8198, 0.7332 and 0.0320. This indicates that an increase in nitric acid concentration causes a similar but weaker effect on droplet concentration as an increase in particle concentration.

## 5. Aerosols, clouds and their climatic impacts

Since the beginning of this century, releases of sulphur species has grown substantially due to human activities. This has also affected atmospheric particle loadings. Increased aerosol particle concentrations increase directly the scattering of solar radiation in the atmosphere. This reduces the amount of solar radiation available at the Earth's surface, and may exert a considerable cooling influence on the climate. Recent progress in the development of more sensitive GCMs has improved their capability to take into account direct aerosol effects: Mitchell *et al.*, (1995) have shown

that inclusion of (direct) sulphate aerosol forcing improves substantially the simulation of the global mean temperature.

One of the major uncertainties in aerosol-climate interaction is the indirect aerosol effect described earlier. The radiative properties of clouds (their optical depth and albedo) depend on their liquid water content and on droplet size distribution (*Twomey, 1977*). The more droplets there are in a cloud, the larger is its albedo at solar wavelengths.

The number and size of droplets in developing clouds depend strongly on the number and hygroscopic properties of pre-existing aerosol particles. The cloud droplet number concentration increases when the number of suitable soluble salt particles (e.g. ammonium sulphate) is greater. Furthermore, as discussed earlier, also some gaseous pollutants (such as various inorganic acids) may affect the number of activated cloud droplets due to the increased amount of hygroscopic matter in the developing cloud condensation nuclei. Measurements have shown that there is a nonlinear relationship between the number of cloud droplets and the concentration of atmospheric pollutants (*Leaitch et al., 1992*).

In addition to increasing scattering, enhanced aerosol particle and cloud droplet concentrations may increase the absorption of solar and terrestrial (infrared) radiation, especially if the amount of elemental carbon in particles is increased (e.g. *Penner et al., 1994*). This may, to some degree, decrease the particle cooling influence. One should thus bear in mind that also absorption of solar and terrestrial radiation is related to aerosol particles and clouds, and that their interaction with atmospheric radiation fluxes is not always straightforward.

The cloud albedo ( $A$ ) and the cloud droplet number concentration ( $N$ ) are related through optical thickness ( $\tau$ ). The cloud albedo can be approximated with following equation (*Lacis and Hansen, (1974)*):

$$A = \frac{\tau}{(7.7 + \tau)} \quad (2)$$

The sensitivity of cloud optical thickness and albedo to changes in cloud droplet concentration at constant liquid water content (kg of cloudwater in m<sup>3</sup> of air) and cloud height is given by

$$\frac{\Delta\tau}{\tau} = \frac{\Delta N}{3N} \quad (3)$$

and

$$\frac{dA}{dN} = \frac{A(1-A)}{3N} \quad (4)$$

Thus for given  $N$  the most susceptible clouds are those with  $A$  around 0.5. However, the maximum of  $A$  is rather flat: for  $A=0.25$  or  $A=0.75$ ,  $dA/dN$  is still about three-fourths of its maximum value (see *Twomey*, 1991).

We have calculated, using equation 4, how optical properties of a cloud layer depend on the increased cloud droplet concentration due to the interaction between pre-existing particles and gaseous nitric and hydrochlorid acid. The change in the cloud optical thickness as a function of the acid concentration (both  $\text{HNO}_3$  and  $\text{HCl}$ ) is presented in Table 1. One can see that in general, the optical thickness and thus also the albedo of a cloud increase with increasing acid concentration, i.e. with increasing soluble mass in the system.

Table 1. The comparison of  $\text{HCl}$  and nitric acid effect on the change of the optical thickness of a cloud.  $\Delta N/3N$  is calculated using the difference between 10 ppbv (or 1 ppbv) nitric acid or  $\text{HCl}$  concentration compared with conditions without acid. The initial conditions were similar in all three cases. The initial bimodal aerosol particle distribution was lognormal, with mean aerodynamic radii of 30 nm (Aitken mode) and 100 nm (accumulation mode) and standard deviations of 1.35 (Aitken mode) and 1.6 (accumulation mode). The initial particle concentrations were  $1000 \text{ cm}^{-3}$  (in the Aitken mode) and  $100 \text{ cm}^{-3}$  (in the accumulation mode). (see also *Kulmala et al.*, 1995a).

System	The change in acid concentration (ppbv)	$\Delta\tau/\tau$
$\text{NaCl-H}_2\text{O-HCl}$	1.0	0.051
	10.	0.145
$\text{NH}_4\text{NO}_3\text{-H}_2\text{O-HNO}_3$	1.0	0.060
	10	0.230
$\text{NaNO}_3\text{-H}_2\text{O-HNO}_3$	1.0	0.060
	10	0.230

We have also estimated the global-mean shortwave forcing due to the effect of nitric acid on cloud droplet concentration using the expression given by e.g. *Charlsson et al.*, 1992 (see also *Schwartz*, 1996).

$$\Delta F_c \approx -0.075(F_T / 4)A_c T^2 \Delta \ln N \quad (5)$$

Here  $F_T$  is the solar constant ( $\sim 1370 \text{ W m}^{-2}$ ),  $A_c$  is the fractional coverage of clouds,  $T$  is the fraction of incident shortwave radiation transmitted by the atmosphere above the cloud layer. Using values given by *Schwartz* (1996) ( $T = 0.76$  and  $A_c = 0.3$ ) and estimating that present acid concentration is two times higher than the natural one, we obtain for the global forcing  $\sim -0.14 - -0.21 \text{ W/m}^2$ .

Although both model predictions and observations of climate variations have improved substantially over the recent years, not least because of the progress in our ability to better understand phenomena related to aerosols and clouds, major uncertainties still exists (for more details see *Penner et al.*, 1994). For example, some studies relying on satellite measurements find higher cloud albedos over the polluted areas in the United States and Asia (*Kim and Chess*, 1993) as one might expect, while

some other studies find no changes in the cloud albedo over the northern hemisphere (e.g. *Schwartz*, 1988). Thus, it is evident that the understanding of the effects of pollutants on the formation of aerosol particles and cloud droplets, and on the atmospheric radiative balance and, hence, on climate, is not yet sufficient.

### *Acknowledgements*

Support of this work by the Academy of Finland is gratefully acknowledged. J.C. Barrett, S.L. Clegg, H.-C. Hansson, K. Hämeri, R. Mattsson, J.M. Mäkelä, L., H. Savijärvi, Y. Viisanen, P.E. Wagner and A.S. Wexler, are acknowledged for helpful discussions and their contribution.

### *References*

- Aalto, P., U. Tapper, P. Paatero and T. Raunemaa, 1990. *J. Aerosol Sci.*, **21**, S159-S162.
- Aalto, P., M. Kulmala and E.D. Nilsson, 1995. *J. Aerosol Sci.*, **26**, S411-412.
- Bodhaine, B.A., 1983. *J. Geophys. Res.*, **88** 10,753.
- Charlson, R.J., J. Langner, H. Rodhe, C.B. Leovy and S.G. Warren, 1991. *Tellus*, **43AB**, 152.
- Charlson, R.J., S.E. Schwartz, J.M. Hales, R.D. Chess, J.A. Coakley Jr., J.E. Hansen and D.J. Hofmann, 1992. *Science*, **255**, 423.
- Charlson, R.J. and T.M.L. Wigley, 1994. *Scientific American*, **2**, 48.
- Coffmann, D.J. and D.A. Hegg, 1995. *J. Geophys. Res.*, **100**, 7147.
- Countess, R.J. and J. Heicklen, 1973. *J. Phys. Chem.*, **77**, 444.
- Curry, J.A., 1995. *Sci. Total Environ.*, **160/161**, 777-791.
- De Santis, F. and I. Allegrini, 1992. *Atmos. Environ.*, **26A**, 3061.
- Eisele, F. L. and D.J. Tanner, 1993. *J. Geophys. Res.*, **98**, 9001.
- Erickson III, D.J., R.J. Ogelsby, S. Marshall, 1995. *Geophys. Res Lett.*, **22;15**, 2017.
- Girshick, S.L. and C.P. Chiu, 1990. *J. Chem. Phys.* **93**, 1273.
- Gras, J.L., 1993. *Atmos. Environ.*, **27A**, 142.
- Hartmann, D.L. and D. Doelling, 1991. *J. Geophys. Res.*, **96**, 869.
- Henry, J.F., A. Gonzales and L.K. Peters, 1983. *Aerosol Sci. Technol.*, **2**, 321.
- Hillamo, R.E. and E.I. Kauppinen, 1991. *Aerosol Sci. Technol.*, **14**, 33.
- Hofmann, D.J., T.L. Deshler, P. Amedieu, W.A. Matthews, P.V. Johnston, Y. Kondo, W.R. Sheldon, G.J. Byrne and J.R. Benbrook, 1989. *Nature*, **340**, 117.
- Hoppel W.A., G.M. Frick, J.W. Fitzgerald and R.E. Larson, 1994. *J. Geophys. Res.*, **99**, 14443.
- IPCC, Ed. by J.J. Houghton, G.J. Jenkins and J.J. Ephraums, 1990. *Climate Change, The IPCC Scientific Assessment*. Cambridge University Press.

- IPCC, Ed. by J.J. Houghton, B.A. Callander and S.K. Varney, 1992. *Climate Change 1992, The Supplementary Report to The IPCC Scientific Assessment*. Cambridge University Press.
- IPCC, Ed. by J.J. Houghton, 1994. *Climate Change 1994*. Cambridge University Press.
- Karlson, R. and E. Ljunström, 1995. *J. Aerosol Sci.*, **26**, 39.
- Kaufman, Y.J. and M.-D. Chou, 1993. *J. Climate*, **6**, 1241.
- Kerminen, V.-M. and A.S. Wexler, 1995a. *Atmos. Environ.*, **29**, 361.
- Kerminen, V.-M. and A.S. Wexler, 1995b. *Atmos. Environ.*, **29**, 3263.
- Kim, Y. and R.D. Chess, 1993. *J. Geophys. Res.*, **98**, 14883.
- Korhonen, P., M. Kulmala and T. Vesala, 1996a. *Atmos. Environ.*, **30**, 1773.
- Korhonen, P., M. Kulmala, H.-C. Hansson, I.B. Svenningsson and N. Rusko, 1996b. *Atmos. Res.*, **41**, 249.
- Kulmala, M., A. Laaksonen, P. Korhonen, T. Vesala, T. Ahonen and J.C. Barrett, 1993. *J. Geophys. Res.*, **98**, 22949.
- Kulmala, M., P. Korhonen, A. Laaksonen and T. Vesala, 1995a. *Geophys. Res. Lett.*, **22**, 239.
- Kulmala, M., V.-M. Kerminen and A. Laaksonen, 1995b. *Atmos. Environ.*, **29**, 377.
- Kulmala M., J. Mäkelä, T.W. Choularton, A. Wiedensohler and H.-C. Hansson, 1995c. *J. Aerosol Sci.*, **26**, S463.
- Kulmala, M., P. Korhonen, T. Vesala, H.-C. Hansson, K. Noone and B. Svenningsson, 1996. *Tellus B*. **48B**, 347.
- Laaksonen, A., V. Talanquer and D.W. Oxtoby, 1995. *Annu. Rev. Phys. Chem.*, **46**, 489.
- Lacis, A.A. and J.E. Hansen, 1974. *J. Atmos. Sci.*, **31**, 118.
- Langner, J. and H. Rodhe, 1991. *J. Atmos. Chem.*, **13**, 225.
- Leitch, W.R., G.A. Isaac, J.W. Strapp, C.M. Banic and H.A. Wiebe, 1992. *J. Geophys. Res.* **97**, 2463.
- Mitchell, J.F.B., T.C. Johns, J.M. Gregory and S.F.B. Tett, 1995. *Nature*, **376**, 501.
- Novakov, T. and J.E. Penner, 1993. *Nature*, **365**, 823.
- Parungo, F., J.F. Boatman, H. Sievering, S.W. Wilkinson and B.B. Hicks, 1994. *J. Climate*, **7**, 434.
- Penner, J.E., R.J. Charlson, J.M. Hales, N.S. Laulainen, R. Leifer, T. Novakov, J. Ogren, L.F. Radke, S.E. Schwartz and L. Travis, 1994. *Bulletin of Amer. Met. Soc.*, **75**, 375.
- Raes, F., 1995. *J. Geophys. Res.*, **100**, 2893.
- Raes F. and R. Van Dingenen, 1992. *J. Geophys. Res.* **97**, 12901.
- Pirjola, L., 1995. Licentiate thesis, University of Helsinki, Department of physics.
- Russell, L.M., S.N. Pandis and J.H. Seinfeld, 1994. *J. Geophys. Res.*, **99**, 20989.
- Schwartz, S.E., 1988. *Nature*, **336**, 441.
- Schwartz, S.E., 1996. In: *Nucleation and Atmospheric Aerosols 1996*, 770, edited by M. Kulmala and P.E. Wagner. Elsevier Science, Oxford.



- Seinfeld, J.H., 1986. *Atmospheric Chemistry and Physics of Air Pollution*. John Wiley & Sons, New York.
- Sheridan, P.J., 1989. *Atmos. Environ.*, **23**, 2371.
- Svenningsson, I.B., H.-C. Hansson, A. Wiedensohler, J.A. Ogren, K.J. Noone and A. Hallberg, 1992. *Tellus*, **44B**, 556.
- Svenningsson, B., H.-C. Hansson, A. Wiedensohler, K. Noone, J. Ogren, A. Hallberg and R. Colvile, 1994. *J. Atmos. Chem.*, **19**, 129.
- Twomey, S., 1977. *J. Atmos. Sci.*, **34**, 1149.
- Van Valin, C.C. and R.F. Pueschel, 1981. *Atmos. Environ.*, **15**, 177.
- Virkkula, A., M. Mäkinen, R. Hillamo and A. Stohl, 1995. *Water, Air and Soil Pollut.*, **85**, 1997.
- Wiedensohler, A., D. Covert, E. Swietlicki, P. Aalto, J. Heintzenberg and C. Leck, 1996. *Tellus*, **48B**, 213.
- Wolfenbarger, J.K. and J.H. Seinfeld, 1990. *J. Aerosol Sci.*, **21**, 227.
- Wurzler, S., A.I. Flossman, H.R. Pruppacher and S.E. Schwartz, 1995. *J. Atmos. Chem.*, **20**, 259.
- Wyslouzil, B.E., J.H. Seinfeld, R.C. Flagan and K. Okuyama, 1991. *J. Chem. Phys.*, **94**, 6842.
- Zhang, X.Q., P.H. McMurry, S.V. Hering and G.S. Casuccio, 1993. *Atmos. Environ.*, **27A**, 1593.